Environment International 214 (2026) 110409

Contents lists available at ScienceDirect

Environment International

journal homepage: www.elsevier.com/locate/envint

Full length article

Assessing global factors associated with tropical cyclone-related mortality: A population-based longitudinal study

Wenzhong Huang [a,b], Zhengyu Yang [b,c], Christian Otto [d], Matthias Mengel [d], Simon Hales [e], Yiwen Zhang [b], Rongbin Xu [f,g], Michelle L. Bell [h], Antonio Gasparrini [i], Haidong Kan [j], Francesco Sera [k], Joel Schwartz [l], Eric Lavigne [m,n], Samuel Hundessa [b], Wenhua Yu [b], Paul Lester Carlos Chua [o], Xerxes Seposo [p,q], Patrick Goodman [r], Ariana Zeka [s], Masahiro Hashizume [o,q], Micheline S. Z. S. Coelho [t], Zhihu Xu [b], Tingting Ye [b], Pei Yu [b,u], Yao Wu [b,v], Bo Wen [b], Yanming Liu [b], Shanshan Li [b], Yuming Guo [b,*], MCC collaborators

[a] Key Laboratory of Environmental Medicine and Engineering of Ministry of Education, and School of Public Health, Southeast University, Nanjing, Jiangsu, China
[b] Climate, Air Quality Research Unit, School of Public Health and Preventive Medicine, Monash University, Melbourne, Australia
[c] Department of Urban Planning and Design, Urban Systems Institute, the Social Infrastructure for Equity and Wellbeing (SIEW) Lab, and the Hong Kong Base of the State Key Laboratory of Subtropical Building and Urban Science, The University of Hong Kong, Hong Kong SAR, China
[d] Potsdam Institute for Climate Impact Research, Potsdam, Germany
[e] Department of Public Health, University of Otago, Wellington, New Zealand
[f] Chongqing Emergency Medical Center, Chongqing University Central Hospital, School of Medicine, Chongqing University, Chongqing 400044, China
[g] School of Public Health and Preventive Medicine, Faculty of Medicine, Nursing and Health Sciences, Monash University, Melbourne, VIC 3004, Australia
[h] School of the Environment, Yale University, New Haven, CT, USA
[i] Environment & Health Modelling (EHM) Lab, Department of Public Health Environments and Society, London School of Hygiene & Tropical Medicine, London, UK
[j] Department of Environmental Health, School of Public Health, Fudan University, Shanghai, China
[k] Department of Statistics, Computer Science and Applications "G. Parenti", University of Florence, Florence, Italy
[l] Department of Environmental Health, Harvard T.H. Chan School of Public Health, Boston, MA, USA
[m] School of Epidemiology and Public Health, Faculty of Medicine, University of Ottawa, Ottawa, Ontario, Canada
[n] Environmental Health Science and Research Bureau, Health Canada, Ottawa, ON, Canada
[o] Department of Global Health Policy, Graduate School of Medicine, The University of Tokyo, Tokyo, Japan
[p] Department of Hygiene, Graduate School of Medicine, Hokkaido University, Sapporo, Japan
[q] School of Tropical Medicine and Global Health, Nagasaki University, Nagasaki, Japan
[r] Technological University, Dublin, Ireland
[s] Institute for Global Health, University College London, London, UK
[t] Department of Pathology, School of Medicine, University of São Paulo, São Paulo, SP 05508-060, Brazil
[u] Guangdong Key Laboratory of Environmental Pollution and Health, College of Environment and Climate, Jinan University, Guangzhou, 511443, China
[v] MEEKL-AERM, College of Environmental Sciences and Engineering, and Center for Environment and Health, Peking University, Beijing, China

ABSTRACT

Background: The underlying factors associated with the substantial global tropical cyclone (TC)-related mortality burden, characterized by its highly variable spatiotemporal patterns, remain unclear. We aimed to identify and assess the key factors associated with TC-related mortality on a global scale.

Methods: We collected mortality records from 2034 locations in 68 countries/territories across five continents (2000–2019) to identify and assess the key factors associated with TC-related mortality on a global scale. Bayesian ensemble models were applied to estimate the associated mortality for each TC event in each location. A random forest regression (RFR) model was employed to assess the relative statistical importance of TC and location characteristics, as well as their interactions, regarding the TC-related mortality.

Findings: For TC physical characteristics, the TC-associated cumulative rainfall consistently exhibited stronger influence on mortality than TC-induced surge-driven flood depth or maximum sustained windspeed. However, sociodemographic factors, including population traits (e.g., population density, proportion of the population aged $\leq$ 9 years, percent of the population aged $\geq$ 65 years) and socioeconomic and infrastructure development (e.g., built-up ratio), showed greater relative importance than the TC physical attributes and accounted for the majority of the explained variations in TC-related mortality. Furthermore, cumulative rainfall

* Corresponding author at: Climate, Air Quality Research Unit, School of Public Health and Preventive Medicine, Monash University, Melbourne, VIC 3004, Australia.

E-mail address: yuming.guo@monash.edu (Y. Guo).

https://doi.org/10.1016/j.envint.2026.110409
Received 12 March 2026; Received in revised form 3 July 2026; Accepted 6 July 2026
Available online 7 July 2026

interacted strongly with local sociodemographic conditions and was potentially the most important associated factor for disparities in mortality arising from factor interactions.

Interpretation: The findings highlight the critical role of sociodemographic factors in explaining the global spatiotemporal variability of TC-related mortality, surpassing the relative importance of TC intensity. TC-related rainfall could be a key associated physical factor of the global mortality burden.

1. Introduction

Tropical cyclones (TCs), including tropical storms, hurricanes and typhoons, are a leading contributor to the global economic burden of natural disasters, ranking as the costliest extreme climate events. Over 2013–2022, TCs affected an average of 20.4 million people per year and caused mean annual direct losses of US$51.5 billion (reported in nominal, event-year US$). (CRED) In the context of global warming, aging populations, and rapidly expanding coastal communities, exposure to such extreme events remains a significant public health concern and a key driver of climate-related hazards. (Knutson et al., 2020; Wang et al., 2022; Reimann et al., 2023).

Recent evidence has demonstrated the persistent mortality (Parks et al., 2023; Young and Hsiang, 2024; Huang et al., 2023; Huang et al., 2024; Parks et al., 2022) and morbidity (Parks et al., 2021; Huang et al., 2024; Salas et al., 2024) risks in the aftermath of TCs. However, despite the well-acknowledged TC-related hazards, the underlying key factors associated with these health risks remain largely unknown, especially on a global scale. The health impacts of TCs can vary considerably depending on the characteristics of the TC events and the vulnerabilities of the affected populations. (Parks et al., 2023; Huang et al., 2024) Understanding the contributions of spatiotemporal variations in TC characteristics, as well as demographic and socioeconomic factors associated with the health effects would help inform understanding of the potential mechanisms by which climate extremes affect public health, which is a key aspect of informing mitigation and prevention strategies. (Prada et al., 2024).

Previous global assessments have provided insights into the regional and socioeconomic disparities in the impacts of TCs. (Jing et al., 2024; Geiger et al., 2021; Ye et al., 2020; Geiger et al., 2018) However, these studies mainly focused on TC exposure levels (e.g., TC frequency) and did not account for the local population health risks associated with TCs. For example, regions with lower TC frequency could exhibit higher mortality risks after TC exposures, potentially due to lower adaptation capacity. (Huang et al., 2025) Epidemiological studies have evaluated local empirical population health risks associated with TCs and potential risk modifiers, but these analyses typically focus on a single or limited set of socioeconomic variables. (Young and Hsiang, 2024; Parks et al., 2022; Huang et al., 2024; Tennant and Gilmore, 2020; Huang et al., 2023) For example, higher TC-associated mortality risks have been reported in regions with lower income levels or greater socioeconomic deprivation. (Tennant and Gilmore, 2020) Such subgroup analyses, however, overlooked the contributions and potential interactions of other factors that may also influence TC health effects, such as variations in TC physical characteristics.

To address these gaps, we collected mortality data spanning two decades from TC-exposed locations in 68 countries and territories, accounting for approximately 42.6% of the global population exposed to TCs. (Jing et al., 2024) These countries and territories represent a wide range of population, socioeconomic and TC characteristics, providing a suitable setting for exploring the key factors associated with TC-related deaths at a global scale. (Gasparrini et al., 2024) We aimed to quantify the relative importance of the TC characteristics, demographic and socioeconomic factors, as well as their interactions, in relation to the empirical local TC-related deaths based on real-world population mortality surveillance data. We sought to identify the key factors associated with TC-related deaths to better understand the health effects of TCs in the context of a changing climate.

2. Methods

2.1. Data collection

We integrated a global dataset of 2034 locations from 68 countries or territories based on a well-established Multi-Country Multi-City (MCC) Collaborative Research Network database that aimed to provide systematic epidemiological evidence on the health impacts of environmental stressors across countries and regions (https://mccstudy.lshtm.ac.uk/). The details of the data collection and organization procedure were provided in Supplementary Text S1. Among these 2034 locations, 413 locations from 23 countries or territories that experienced at least 1 TC during the study period were included in the subsequent analysis. These locations represented approximately 42.6% of the global population exposed to TCs. (Jing et al., 2024) More information and descriptive statistics of these included locations are displayed in Table S1.

We selected a series of potential factors associated with TC-related mortality to represent five key dimensions that have been implicated in prior research on cyclone-related health impacts (Huang et al., 2023; Doocy et al., 2013): (1) TC physical characteristics (windspeed, rainfall, storm surge); (2) demographic and population traits (population size, population density, percent of the population aged $\geq$ 65 years, percent of the population aged $\leq$ 9 years, percent of female population); (3) local socioeconomic (i.e., socio-demographic index [SDI], the ratio of built-up area to the non-built-up area [Built-up ratio]); (4) governance and healthcare levels (regulatory quality, government effectiveness, healthcare access and quality [HAQ]); and (5) climatic context (Köppen-Geiger climate zones). Factor selection within each dimension was guided by the availability of longitudinal data that provided sufficient spatiotemporal coverage to support our global, multi-site analysis, focusing on variables that are routinely measured and comparable across countries. Detailed information on each factor (e.g., sources, definition, spatiotemporal resolution, and organization procedure) is provided in Table S2.

2.2. TC-associated windspeed, rainfall and surge-driven flood depth assessment

To estimate the population center of each location for exposure assessment, we used annual population count data at 0.01° spatial resolution across the globe during the years 2000–2019 from LandScan. (Dobson et al., 2000) The population data were first calibrated annually for each country and territory to ensure consistency with United Nations population estimates, as detailed in our previous work. (Xu et al., 2023) Subsequently, for each location and year, we calculated the population-weighted centroid based on the calibrated grid-specific population counts within each location. Given the unavailability of high-resolution population data prior to 2000 for estimating population centroids and demographic factors associated with TC-related mortality, we focused on TC exposures from the year 2000 onward.

We used the Holland model (Holland et al., 2010), the most widely used TC hazard model (Geiger et al., 2021; Peduzzi et al., 2012; Lange et al., 2020); to estimate the wind fields for each historical TC event. The methodology of this model was described in detail in our previous work (Huang et al., 2023; Huang et al., 2024; Geiger et al., 2018). Briefly, a parametric wind field model was implemented using global cyclone characteristic data from the International Best Track Archive for Climate Stewardship (IBTrACS) (Knapp et al., 2010) to produce global gridded daily maximum sustained wind speeds associated with each cyclone event in the IBTrACS database. Wind speeds were initially estimated at a spatial resolution of 5 arcminutes (1/12°, approximately 10 km × 10 km at the equator) and an hourly temporal resolution. These estimates were subsequently averaged and aggregated to a spatial resolution of 0.5° and a daily temporal resolution, adjusted to local time zones. For each location, a TC exposure day was defined as a day on which the TC-associated maximum wind speeds at the population centroid reached or exceeded 17.5 m/s. (Parks et al., 2022; Parks et al., 2021) Furthermore, we extracted the TC-associated rainfalls from the ISIMIP3a dataset, which had a spatial resolution of 5 arcminutes and was derived from a physics-driven TC rainfall model. (Zhu et al., 2013; Frieler et al., 2024) We calculated the TC-associated cumulative rainfalls by summing the grid-level values across all grid cells within each TC-exposed grid on TC exposure days. Finally, as detailed in previous work (Vogt; et al., 2024); the maximum flood depth driven by the TC-induced surge was estimated for each TC event at a spatial resolution of 5 arcminutes using the GeoClaw adaptive mesh shallow water solver integrated within CLIMADA (https://github.com/CLIMADA-project/climada_python). The generated flood depth data are publicly available at Zenodo (https://zenodo.org/records/14547984). These flood depth estimates were then averaged and aggregated to a 0.5° grid resolution, and the exposure of each TC event for each location was assigned based on the value of the grid cell containing that location's population centroid. We aggregated wind speed and surge-driven flood depth as their maximum values at the population centroid because they were localized, peak-intensity forces, allowing the model to capture the maximum intensity experienced by the concentrated population. (Massarra et al., 2019) Rainfall was aggregated as the sum of rainfall (i.e., cumulative rainfall) across exposed grid cells because it represented a cumulative volume hazard that drained into broader catchment basins, which better captured the total hydrological load impacting the area. (Hermans et al., 2024).

3. Statistical analysis

3.1. TC-associated mortality estimation

A two-stage analytical framework was adopted in this study. In the first stage, we implemented Bayesian ensemble models to estimate TC-related mortality, using the same modeling strategies and settings as those detailed and validated in previous studies. (Parks et al., 2023; Kontis et al., 2020) Briefly, for each TC-exposed location, we trained Bayesian ensemble models on the periods of time without TC exposure to estimate the weekly all-cause deaths for the week of and two weeks after exposure had the cyclone not occurred (i.e., the counterfactual number of deaths). Mortality data were aggregated weekly to enhance the stability of the analysis (since narrower time intervals led to smaller counts and instability in the time series for many locations) (Parks et al., 2022; Kontis et al., 2020), while retaining the ability to capture finer temporal variations (Ebi, 2024). We focused on the two-week post-TC period because (1) extending the exposure window would substantially increase uncertainty in estimating TC-related mortality for the Bayesian ensemble models based on weekly analyses, and (2) our previous work at a multi-country level suggested that the mortality risks associated with TCs decline rapidly after exposure and tend to be modest beyond this timeframe (Huang et al., 2023; Huang et al., 2025). A longer hypothetical exposure window may also introduce a higher risk of bias by capturing longer-term changes unrelated to the TC. (Nethery et al., 2023) For each location, the associated mortality of each TC event was calculated as the difference between the observed number of deaths from all causes and the counterfactual number of deaths.

The Bayesian ensemble models included 16 predictive models with different options to account for temporal trends, autoregression, and temperature effects, as detailed previously. (Kontis et al., 2020) Briefly, by assuming a Poisson distribution for the number of weekly deaths (also accounting for possible overdispersion), these models included predictors including long-term temporal trends, seasonal patterns, relation to immediately preceding weeks (i.e., autoregression), temperature anomalies and population offset to estimate the counterfactual deaths. There were two settings for long-term trends (one assuming no trend and one with a linear trend term over weekly deaths), four settings for the autoregressive term using different orders (first, second, fourth, or sixth) and two settings for temperature anomalies (one without temperature and one with terms to account for temperature anomaly). These combinations resulted in an ensemble of 16 Bayesian models (2 trend options × 4 autoregressive options × 2 temperature options).

Multiple models were used to account for the inherent uncertainty in selecting the best model for predicting the counterfactual deaths for each location. A model-averaging approach can improve the overall prediction accuracy. (Graefe et al., 2015) We averaged the predictions from the 16 models in the ensemble by their predictive accuracy, as with previous studies. (Parks et al., 2023; Graefe et al., 2015) The number of draws taken from each model's posterior distribution of deaths was proportional to the inverse of the percentage error, with a minimum of 0 and a maximum of 1000 draws.

3.2. Evaluation key factors associated with TC-related mortality

In the second stage, we used a random forest regression (RFR) model to assess the relative statistical importance of the location and TC characteristics in explaining TC-associated mortality. Compared to traditional models (e.g., linear regression models), RFR models can effectively capture potential non-linear effects and complex interactions among variables while maintaining robustness against overfitting. (Liu et al., 2021; Ronco et al., 2023; Zhou et al., 2023) Because our primary objective was exploratory (i.e., descriptions of relative importance for various factors, without a factor of pre-defined priority), we did not use causal forest methods, which were recently developed to estimate the causal effect of a treatment/intervention variable within the generalized random forest framework and require a single, pre-defined treatment/intervention factor with priority. (Tibshirani et al., 2025).

In the RFR models, we used an ensemble of 1000 trees (ntree = 1000), which was chosen because further increases in ntree produced negligible reductions in the out-of-bag error (a proxy for performance on unseen data). Another parameter, the number of candidate variables considered at each split (mtry), was determined by grid search (mtry = 2–10) and the value with the lowest out-of-bag error (mtry = 5) was selected. A total of 14 factors that may influence TC-related deaths were incorporated in the model, including TC-associated maximum sustained windspeed, cumulative rainfall and surge-driven maximum flood depth, SDI, population size, population density, built-up ratio, percent of the population aged $\geq$ 65 years, percent of the population aged $\leq$ 9 years, percent of female population, regulatory quality, government effectiveness, HAQ, and Köppen-Geiger climate zones.

To evaluate the relative statistical importance of these factors in explaining TC-related deaths, we first used three indicators derived from the RFR model splitting behavior: minimal depth across forest trees, root node frequency, and total number of trees where a split occurs. (Paluszynska et al., 2017) Specifically, minimal depth across forest trees reflects the average depth at which a factor first appears as a splitting variable in the decision trees within the forest. A smaller minimal depth indicates that the factor is highly influential, as it is selected early in the decision-making process of the model. Root node frequency measures how often a factor is used as the splitting variable at the root node of the decision trees. A higher root node frequency suggests that the factor has a stronger overall influence on the model and is prioritized in initial splits. The total number of trees where a split occurs represents the number of trees in which a particular factor is used for splitting at any node, regardless of its position in the tree. A higher count indicates that the factor consistently contributes to the model's decisions across the entire ensemble of trees.

To quantify the relative importance while accounting for the uncertainty, we estimated the reduced model performance (i.e., percent increase in the MAE) for each factor when the factor's information is removed by random permutation. (König et al., 2020) Specifically, we recorded a baseline MAE from the RFR model, then repeated the following procedure 1,000 times for each factor: (i) randomly permute the factor's values across observations (preserving its marginal distribution but breaking its association with the outcome and other factors); (ii) compute the MAE of the trained model on the permuted data; and (iii) calculate the percent increase in MAE relative to the baseline (i.e., %ΔMAE). The 1,000 repeated permutations produced an empirical distribution of %ΔMAE for each factor; we report the mean %ΔMAE and the 95% confidence intervals (2.5th-97.5th percentiles) as measures of central tendency and uncertainty when comparing the factors' relative importance.

Moreover, we applied Shapley additive explanations (SHAP) to further decompose and interpret the constructed RFR model by calculating SHAP values for each factor included in the model. (Lundberg et al., 2020; Deng et al., 2025) SHAP values represent the contribution of individual features to the model output, while accounting for potential interactions and nonlinear relationships with other variables. (Lundberg and Lee, 2017) By examining the patterns of SHAP values, we were able to gain more detailed insights into the influence of each factor. Specifically, SHAP dependence plots that illustrate how variations in each factor affect model outputs were used to derive exposure-importance response curves.

Finally, impurity-based importance, a commonly used alternative measure of feature importance, was extracted from the RFR model as the total decrease in node impurity (IncNodePurity) attributed to splits on each factor, summed across all trees. (Voges et al., 2023) For regression trees node impurity was the residual sum of squares, and larger values indicated a greater cumulative reduction in impurity resulting from splits on that variable. To facilitate comparison across approaches and quantify the relative contribution, each factor's importance measures from the three methods (i.e., permutation-based %ΔMAE, impurity-based IncNodePurity, and SHAP-based absolute contributions) were converted into a percentage share by dividing each factor's value by the sum of values across all factors and multiplying by 100.

To test the robustness of our results, we conducted the following sensitivity analysis by excluding the locations in Europe (i.e., the UK, Portugal, Ireland, Spain, and Iceland) and reran the models because North Atlantic TCs typically undergo extratropical transition into mid-latitude storms after European landfall—an evolution that would reduce the accuracy of our wind-field and rainfall simulations, even though these extra-tropical transitions contribute to the TCs' overall, lasting impacts. In addition, because the used parametric wind field models did not capture terrain-induced asymmetries in wind speeds after landfall, we performed sensitivity analysis using a newly developed global TC wind field dataset (Liu et al., 2025). Unlike conventional parametric models, this dataset applies a proportional correction to ERA5 reanalysis data. This approach enhances peak TC wind intensities while preserving the dynamically resolved spatial structure of the original ERA5 wind field, thereby implicitly accounting for the effects of complex topography and surface roughness. Finally, to evaluate the impact of uncertainty from the first-stage mortality estimation on the variable importance assessment in the second-stage RFR model, we conducted a Monte Carlo sensitivity analysis. Specifically, we generated 500 independent simulated datasets of excess mortality by randomly sampling from a normal distribution. This normal distribution was constructed based on the posterior mean and the standard deviation derived from the posterior distributions of our first-stage mortality estimates. We then re-ran the complete RFR model for each of the 500 simulated datasets and evaluated the distributional stability of the variable importance rankings.

All analyses were performed in R software (version 4.4.1), using the R packages "INLA" (Lindgren and Rue, 2015) for the first-stage analysis and "randomForest" (Breiman et al., 2018) and "randomForestExplainer" (Paluszynska et al., 2017) for the second-stage analysis.

4. Results

4.1. Descriptive statistics

A total of 38,793,906 deaths in 413 locations that experienced at least one TC day (days with TC-associated maximum wind speeds ≥ 17.5 m/s) during the study period across 23 countries or territories were included in the analysis (Table S1). The geographical locations and the corresponding TC exposure frequency and characteristics (i.e., TC-associated windspeed, rainfall and storm surge) are shown in Fig. 1 and Fig. 2. A total of 264 TC events affecting these 413 locations were included in the analysis, with their best-track routes also depicted in Fig. 1. The TC exposure frequency varied substantially by location. TCs were most frequently (>30 days per decade) observed for locations in Taiwan, Japan, the USA and the Philippines, and less frequently (<5 days per decade) for locations in Canada, Brazil and New Zealand.

4.2. The estimated TC-related mortality

The root mean squared error (RMSE) of the developed ensemble Bayesian models in estimating location-level weekly deaths is shown in Table S3. The average RMSE ranges from 1.80 (standard deviation [SD]: 0.75) to 13.18 (SD: 3.09) deaths across different countries and territories, with an overall average RMSE of 5.02 (SD: 3.70) deaths. Fig. S1 presents the posterior probability of excess deaths following TC events for each location. Regions with higher TC frequencies (e.g., East and Southeast Asia, and the southeastern USA) consistently exhibited greater posterior probabilities of excess mortality ($P > 0.8$). Notably, the most severe individual TC events resulted in mortality estimates exceeding 200 deaths, as demonstrated by several events in Japan, the Philippines, Taiwan, and the USA (Fig. 3).

4.3. Relative importance of potential factors associated with TC-related mortality

A total of 14 potential associated factors of TC-related deaths were included in the RFR model, which achieved an out-of-bag R^2 of 31.4%. The geographical distributions of these included factors among the TC-exposed locations across the study countries and territories are shown in Figs. S2–S13 and Table S4. Fig. 4a depicts the distribution of the minimal depth across decision trees for these variables, with the mean indicated by a vertical black bar. SDI, population size and density showed much smaller mean minimal depth compared to other factors, suggesting their higher relative importance in explaining the variance in TC-related mortality. These factors, along with other population traits (e.g., the percent of population aged ≤ 9 years, and percent of population ≥ 65 years) and infrastructure development (i.e., built-up ratio), exhibited higher importance ranking based on mean minimal depth compared to physical TC characteristics (i.e., TC-associated wind speed, rainfall, and storm surge). In contrast, climate zones showed much higher mean minimal depth compared to all other factors, indicating their minimal relative statistical importance in explaining TC-related mortality.

Similar patterns were observed in a multiway importance plot combining indicators of root node frequency, mean minimal depth, and total number of trees where a split occurs (Fig. 4b). SDI, population trait indicators, and built-up ratio generally exhibited higher relative statistical importance (i.e., a combination of greater root node frequency, smaller mean minimal depth and a higher total number of trees where a split occurs) compared to other factors. Notably, among TC exposure characteristics, cumulative rainfall exhibited potentially higher statistical importance than maximum sustained windspeed and maximum flood depth based on these three importance indicators. The results

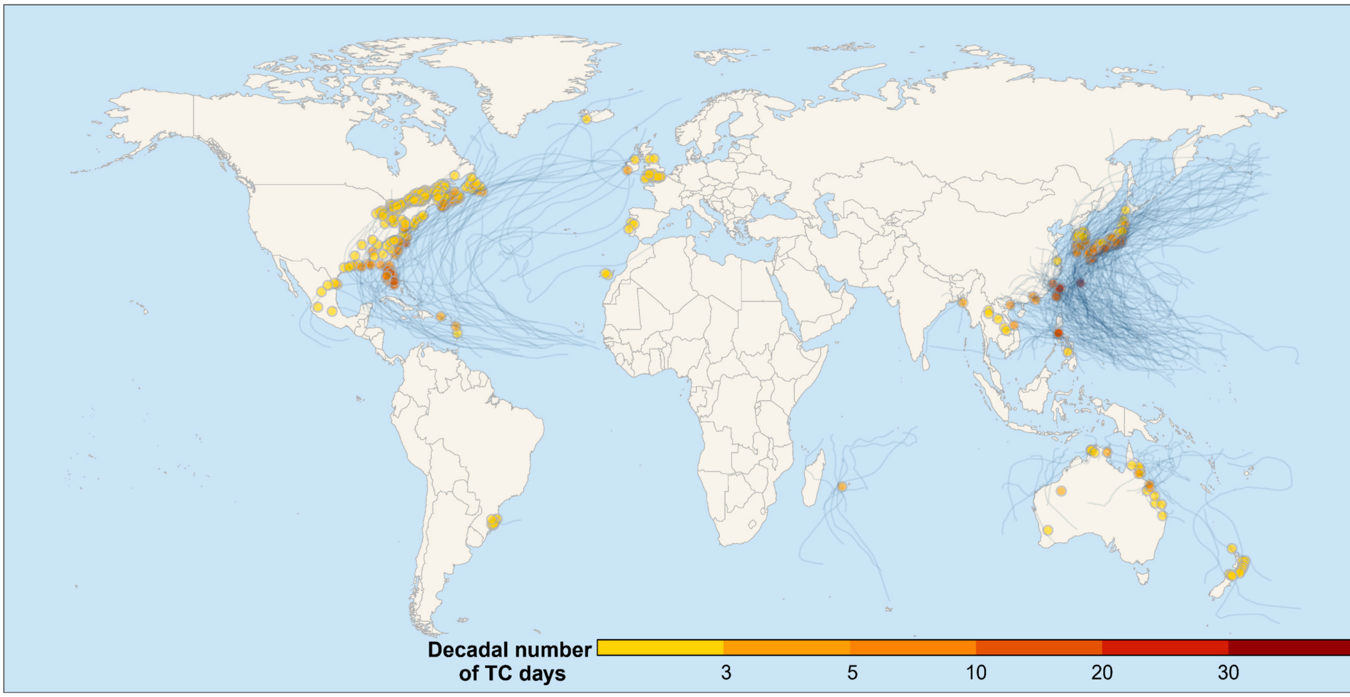

Fig. 1. Geographical locations of the 413 TC-exposed sites in 23 countries or territories included in the study and the corresponding number of TC exposure days per decade during the study period. TC exposure day was defined as a day on which the TC-associated maximum wind speeds at the population centroid were $\geq$ 17.5 m/s for each location. The lines represent the best-track routes of TCs. Abbreviations: TC, tropical cyclone.

remain consistent after excluding European locations (25 out of 413 locations; Fig. S14) or using TC wind field data that accounts for terrain-induced wind field asymmetries (Fig. S15). Furthermore, the robustness evaluation utilizing 500 Monte Carlo simulations demonstrated that the variable importance rankings maintained high distributional stability after accounting for the uncertainty from the first-stage mortality estimation (Fig. S16). Core socio-demographic factors, including the SDI, percent of population aged $\leq$ 9 years and population density, consistently occupied the top ranks with minimal fluctuation. Regarding the key physical characteristics, cumulative rainfall predominantly outranked maximum sustained windspeed, particularly in root node frequency, which reflects a variable's foundational predictive power at the initial splits of the decision trees.

4.4. Relative shares of factors in explaining TC-related mortality

The percent increase in MAE for the RFR model after random permutation of each factor is shown in Fig. 5a. Among TC physical characteristics, permuting cumulative rainfall resulted in the largest median increase in MAE, followed by maximum sustained windspeed and maximum flood depth, indicating that removing rainfall exposure information contributes more to model error than windspeed or storm surge. Population characteristics (in particular population density) and built-up ratio produced the largest increases in MAE of all factors, exceeding the contributions of TC physical characteristics to model performance.

Cumulative rainfall consistently showed a highest share of relative importance among TC physical factors across contribution assessments based on SHAP values, impurity measures, and permutation importance (Fig. 5b). Compared to the TC physical variables, population traits and socioeconomic development indicators exhibited much higher relative contributions, which consistently account for the majority of the importance influencing TC-related mortality across various importance metrics.

4.5. Dominant interacting factors associated with TC-related deaths

We further assessed the relative importance of the interactions among SDI, population density, built-up ratio, percent of the population aged $\leq$ 9 years, HAQ, and TC characteristics (Fig. 6a). Overall, the most important interactions involved TC physical characteristics (i.e., rainfall, windspeed and flood depth) with SDI and population density. Specifically, the interaction between TC-related cumulative rainfall and SDI, with TC-related cumulative rainfall as the root factor, was both the most frequent interaction in the model and the one with the smallest mean conditional minimal depth. This suggested that their combined effects had the greatest relative importance in explaining TC-related deaths. Furthermore, the relative importance of TC-related cumulative rainfall in explaining the associated deaths is closely related to the SDI of the affected population.

4.6. Exposure-importance curve for TC physical characteristics

When examining the exposure-importance response curves for TC exposure characteristics and mortality, all three exposures displayed clear positive exposure-importance relationships, with greater exposures associated with increased importance in explaining TC-related mortality (Fig. 6b–d). Maximum sustained windspeed and surge-driven flood depth exhibited approximately linear exposure-importance response curves. In contrast, the cumulative rainfall curve demonstrated a potential non-linear pattern, with a suggestive threshold effect at around 300 mm of TC-associated weekly cumulative rainfall (Fig. 6b). The distribution of points suggested a pattern where higher SHAP values tended to cluster in lower-SDI settings, indicating that these factors may have greater statistical importance for mortality in locations with lower socioeconomic development.

5. Discussion

Using a large population-based dataset at a global scale, this study is, to the best of our knowledge, the first to systematically evaluate the role

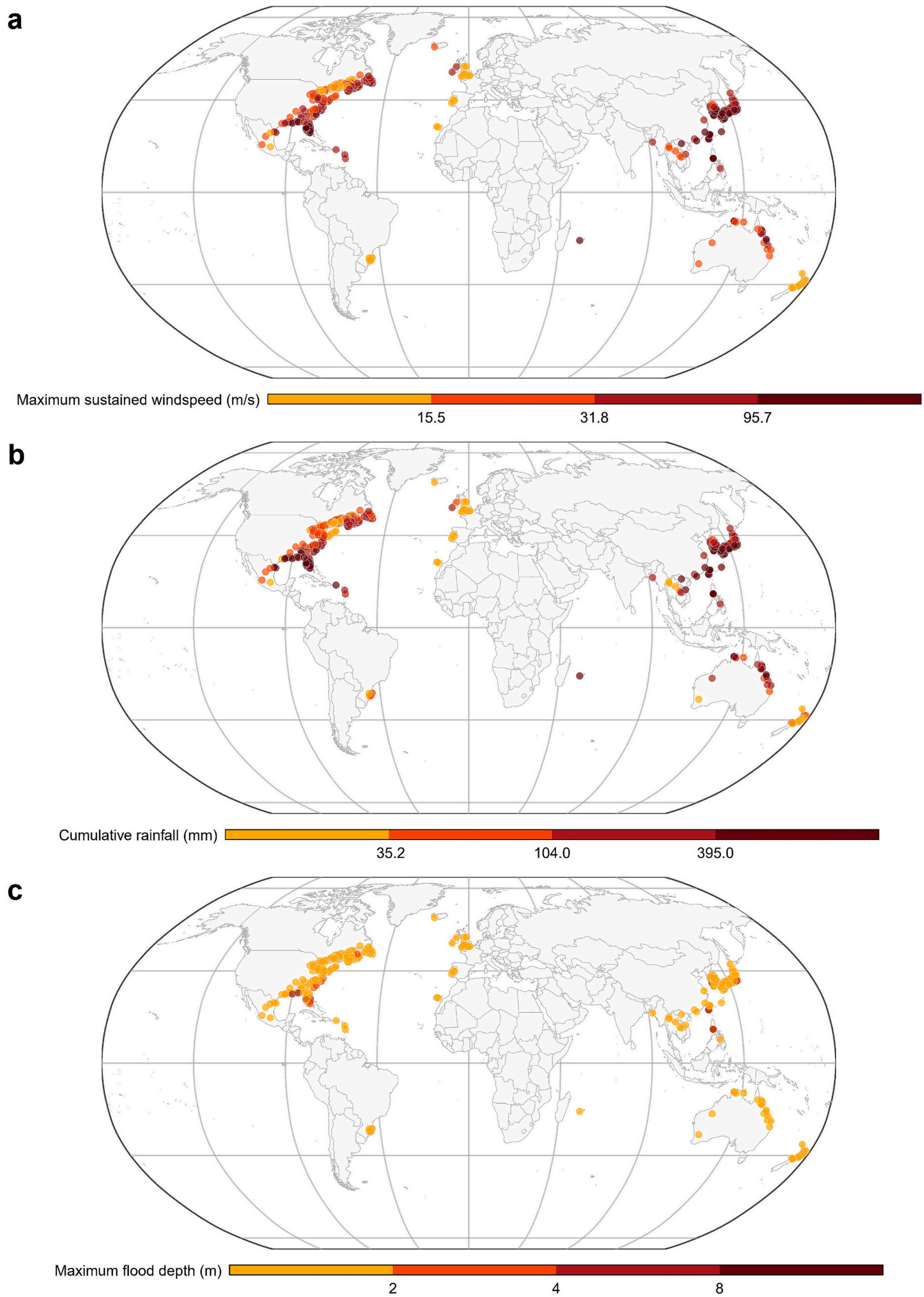

Fig. 2. The decadal cumulative TC-associated maximum sustained windspeed (a), cumulative rainfall (b), and surge-driven maximum flood depth (c) over TC exposure days in the 413 TC-exposed locations across 23 countries/territories during the study period. Abbreviations: TC, tropical cyclone.

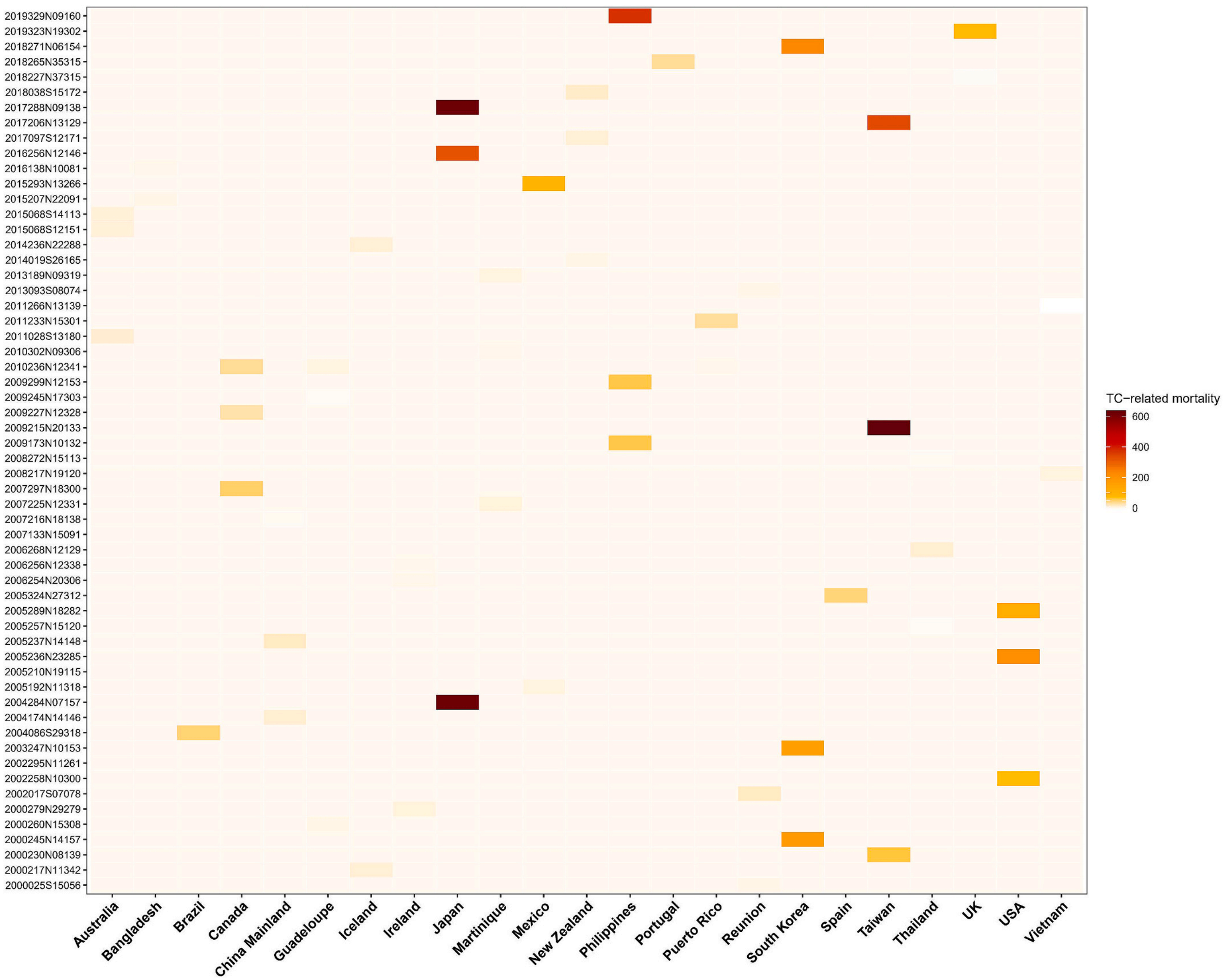

Fig. 3. Total estimated TC-related mortality for the three deadliest TCs in each country and territory. Deaths were summed across all study locations within each country and territory for each TC event, identified by event ID from IBTrACS (y-axis). Abbreviations: IBTrACS, International Best Track Archive for Climate Stewardship; TC, tropical cyclone.

of a wide range of direct and contextual factors in explaining the TC-related mortality burden. Socio-demographic factors were found to be the primary factors associated with local TC-related mortality, surpassing the relative importance of TC physical characteristics. Among TC characteristics, cumulative rainfall was observed to be the most important factor associated with TC-related mortality, followed by TC-induced maximum sustained windspeed and surge-driven flood depth. The combined effects of TC physical characteristics (in particular cumulative rainfall) and socioeconomic development could be the most critical associated factors regarding TC-related mortality.

To date, evidence on the factors associated with the TC-related mortality burden remains scarce, particularly at a multi-country scale. Most existing studies focused on revealing the health risks of TCs, primarily the elevated mortality risks after TCs in the United States. (Parks et al., 2023; Young and Hsiang, 2024; Parks et al., 2022; Huang et al., 2023) These studies have provided partial insights into the factors influencing TC-related mortality by describing the risks by subgroups of a single or a limited number of demographic or socioeconomic factors, such as age, income level, and social vulnerability. (Parks et al., 2023; Parks et al., 2022; Huang et al., 2024; Huang et al., 2023; Liu et al., 2023) Generally higher risks were reported among older populations (Parks et al., 2022) and those with lower incomes (Huang et al., 2024; Dresser et al., 2016) or greater social vulnerability (Parks et al., 2022). One relevant global investigation focused on the role of government effectiveness in explaining country-level TC-related deaths and found it to be a protective factor independent of income level. (Tennant and Gilmore, 2020) However, how these relevant contextual factors, including the physical characteristics of TCs, collectively modify the risks and their relative importance, is not directly available from existing studies. Such evidence represents a critical advancement beyond risk characterization and is essential for a deeper understanding of the health impacts of TCs.

For TC physical characteristics, our analyses provide suggestive evidence that TC-associated cumulative rainfall is a more prominent explanatory factor for mortality than either maximum sustained windspeed or storm surge. This is consistent with our previous work examining the relationships between TC-related windspeed and rainfall with cause-specific mortality across nine countries and territories, which found that TC-related rainfall could be a stronger mortality risk indicator than windspeed, especially for respiratory, cardiovascular, and infectious disease-related deaths. (Huang et al., 2025) The present study, which included TC and all-cause mortality data from 68 countries/territories supported this finding on a global scale. Historically, global TC risk assessments and widely used hazard classifications (e.g.,

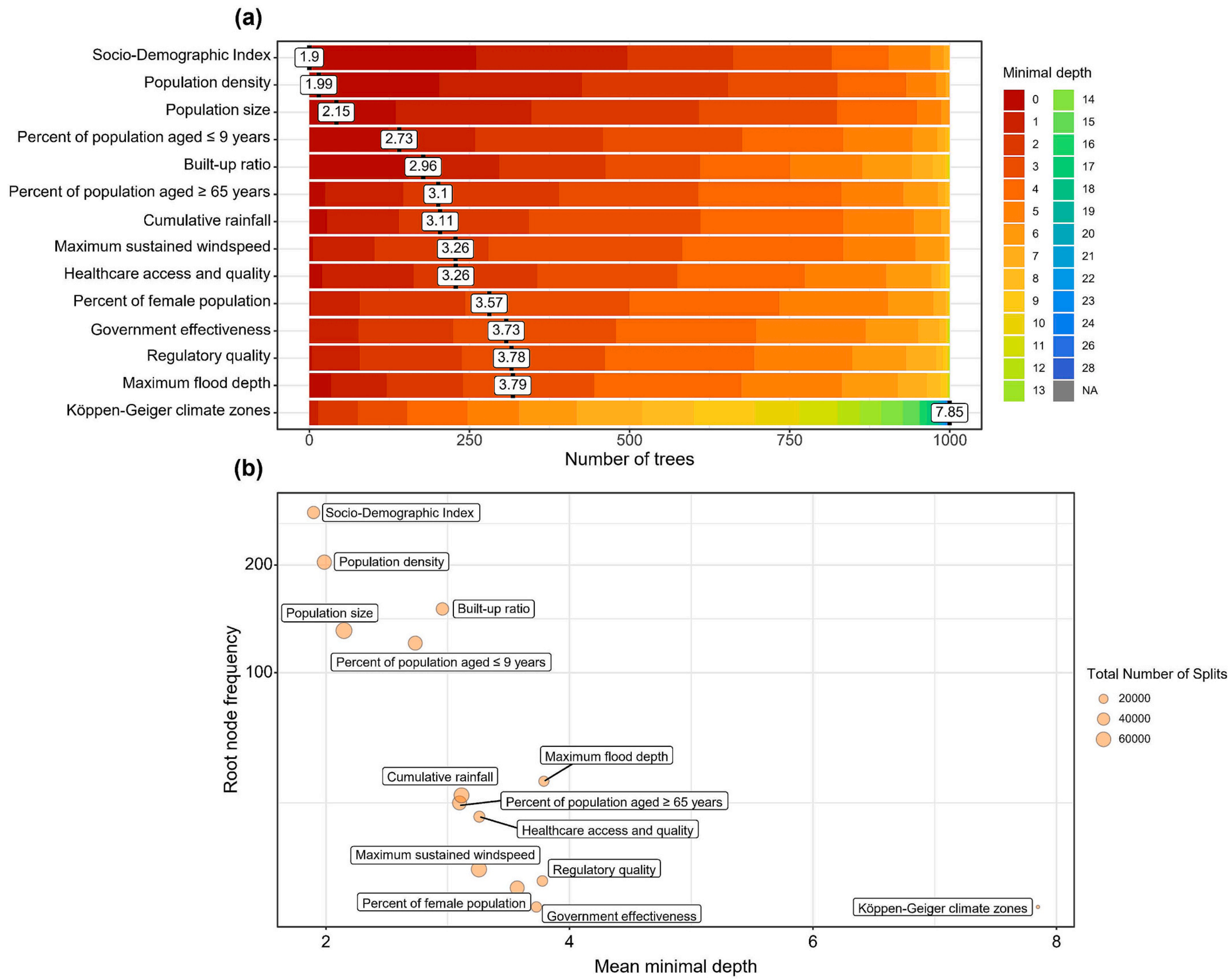

Fig. 4. Relative importance of the included potential factors associated with TC-related deaths. a, distribution of the minimal depth across forest trees for the study variables, with the mean indicated by a vertical black bar and its value labelled. b, multiway importance plot combining root node frequency, mean minimal depth, and total number of trees where a split occurs for each included factor. Minimal depth reflects the average depth at which a factor first appears in the decision trees, with a smaller value indicating higher relative statistical importance. Root node frequency measures how often a factor is used at the root node, with a higher frequency suggesting greater overall explanatory importance. The total number of trees where a factor is used for splitting indicates its consistent explanatory contribution across the ensemble, with a higher count showing more frequent involvement in model decisions. Abbreviations: Built-up ratio, ratio of built-up area to non-built-up area; TC, tropical cyclone.

the Saffir-Simpson hurricane wind scale) have heavily prioritized TC windspeed as the primary indicator of potential severity. However, our findings challenge this traditional wind-centric paradigm on a global scale. These findings suggest that TC-related rainfall intensity warrants greater consideration alongside windspeed in early-warning frameworks, hazard classification schemes and disaster-management planning.

Furthermore, rainfall was identified as a critical TC characteristic that interacts with SDI, demonstrating the highest relative importance regarding the TC mortality disparities. Compared to wind and storm surge, the impacts of TC rainfall are often more extensive and prolonged, causing widespread flooding, landslides, water contamination, and infrastructure damage that can persist long after the storm. (Rappaport, 2014; Bosma et al., 2020; Bosma et al., 2020) These effects can increase TC-related mortality, particularly in socially disadvantaged communities and populations with poor infrastructure, reduced disaster preparedness and response capacity. (He et al., 2024; Yang et al., 2023) Studies have shown that heavy TC-associated rainfall is a leading driver of severe freshwater flooding, which can become the predominant cause of mortality during intense TCs. (Huang et al., 2024; Vosper et al., 2023) The extensive and lingering nature of these rainfall-induced hazards could disproportionately impact the marginalized populations. For example, extensive flooding can lead to the interruption of critical transport routes, water supply contamination and subsequent outbreaks of waterborne diseases, which under-resourced local healthcare systems in low-SDI areas are ill-equipped to manage. In addition, populations in disadvantaged settings tend to reside in substandard housing that is highly susceptible to prolonged water damage and structural collapse, which could exacerbate the long-term hazards of the floodwaters. Consequently, the combination of extreme rainfall and low socioeconomic capacity creates compounding hazards from physical exposure, infrastructural failure, and reduced healthcare access, thereby widening mortality disparities. (Young and Hsiang, 2024; Huang et al., 2024).

Our findings indicated that socio-demographic factors, including economic development, population traits, and built-up ratio, could be the primary explanatory factors for TC-related mortality, surpassing the

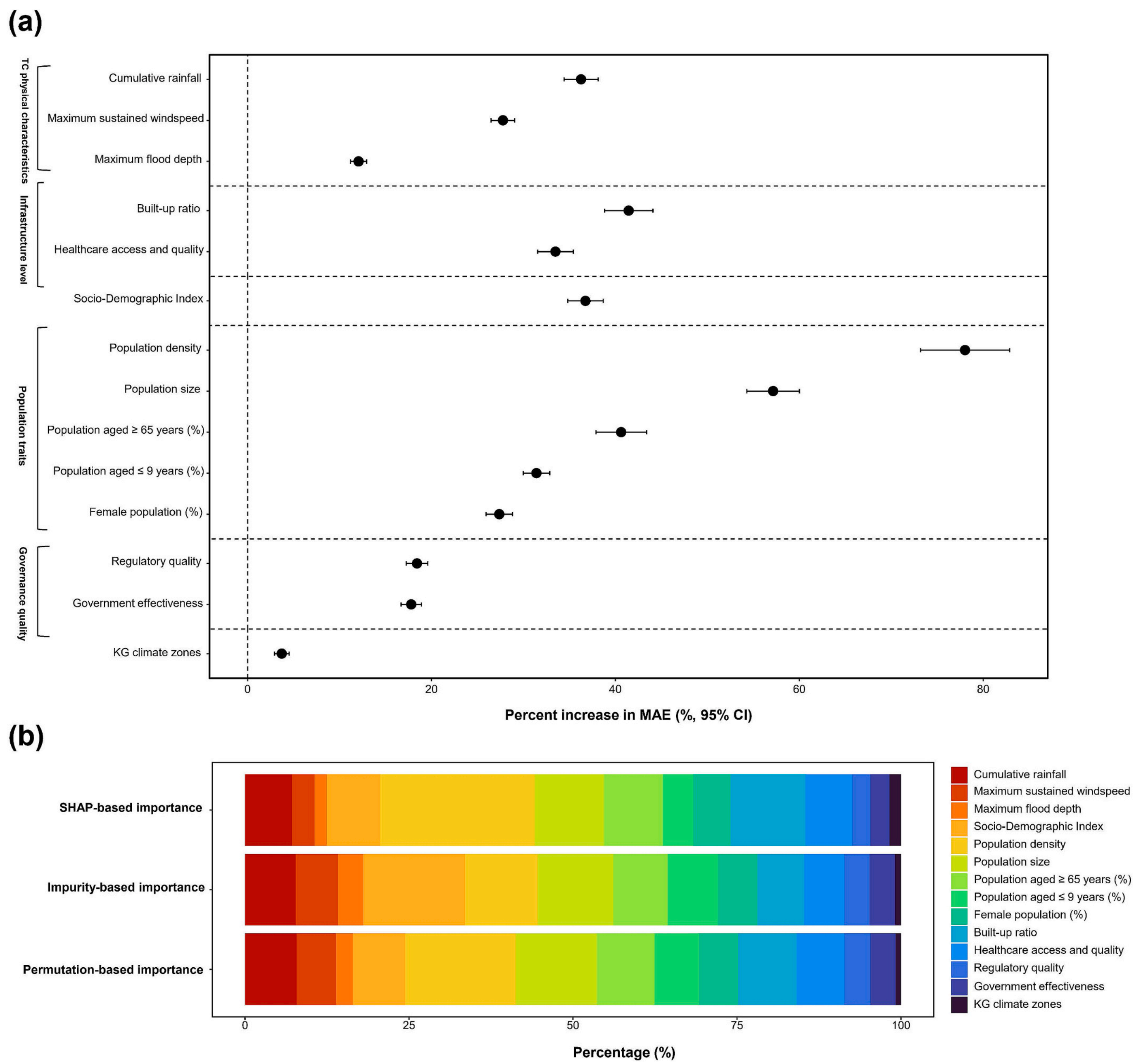

Fig. 5. Percent increase in the MAE for each included potential associated factor after permutation (a) and relative statistical importance of each factor regarding TC-related deaths (b). Points and error bars in panel (a) show the distribution of the percent increase in MAE with the mean and its 95% CI derived from 1,000 random permutations for each factor in RFR model. In panel (b), SHAP-based contribution plot showing each factor's share of the total absolute SHAP contribution (percent); impurity-based importance represents the proportion of total reduction in node impurity (residual sum of squares) attributed to each factor across all trees; permutation-based importance measures the average increase in MAE when the values of a given factor are randomly permuted, repeated 1000 times. Abbreviations: Built-up ratio, ratio of built-up area to non-built-up area; CI, confidence interval; RFR, random forest regression; TC, tropical cyclone; MAE, mean absolute error; SHAP, SHapley Additive exPlanations.

relative statistical importance of physical cyclone characteristics (i.e., rainfall, windspeed and storm surge). This underscored the critical role of underlying social vulnerability and community development in explaining variations in health outcomes following TC exposure. Reducing cyclone mortality may require more than advancements in meteorological forecasting. Disaster management strategies that address population vulnerabilities (e.g., through targeted preparedness, resilient infrastructure and equitable access to healthcare protection) (Huang et al., 2023; Wolkin et al., 2015; Pratiti, 2023) could potentially achieve larger reductions in cyclone-related mortality compared to interventions focused solely on the physical hazards. Furthermore, this highlights the necessity of integrating socio-demographic data into TC early-warning systems, evacuation planning, and resource pre-positioning, which could more effectively improve outcomes and mitigate TC-related health burden.

Our study had several strengths. While prior research has established broad associations between cyclone-related mortality and factors such as socio-demographic vulnerability and rainfall-related hazards, our study provides new evidence and insights in three key ways. First, unlike previous global assessments that commonly rely on officially reported direct loss figures, which are often subject to regional reporting inconsistencies or political influences, our estimations are derived from

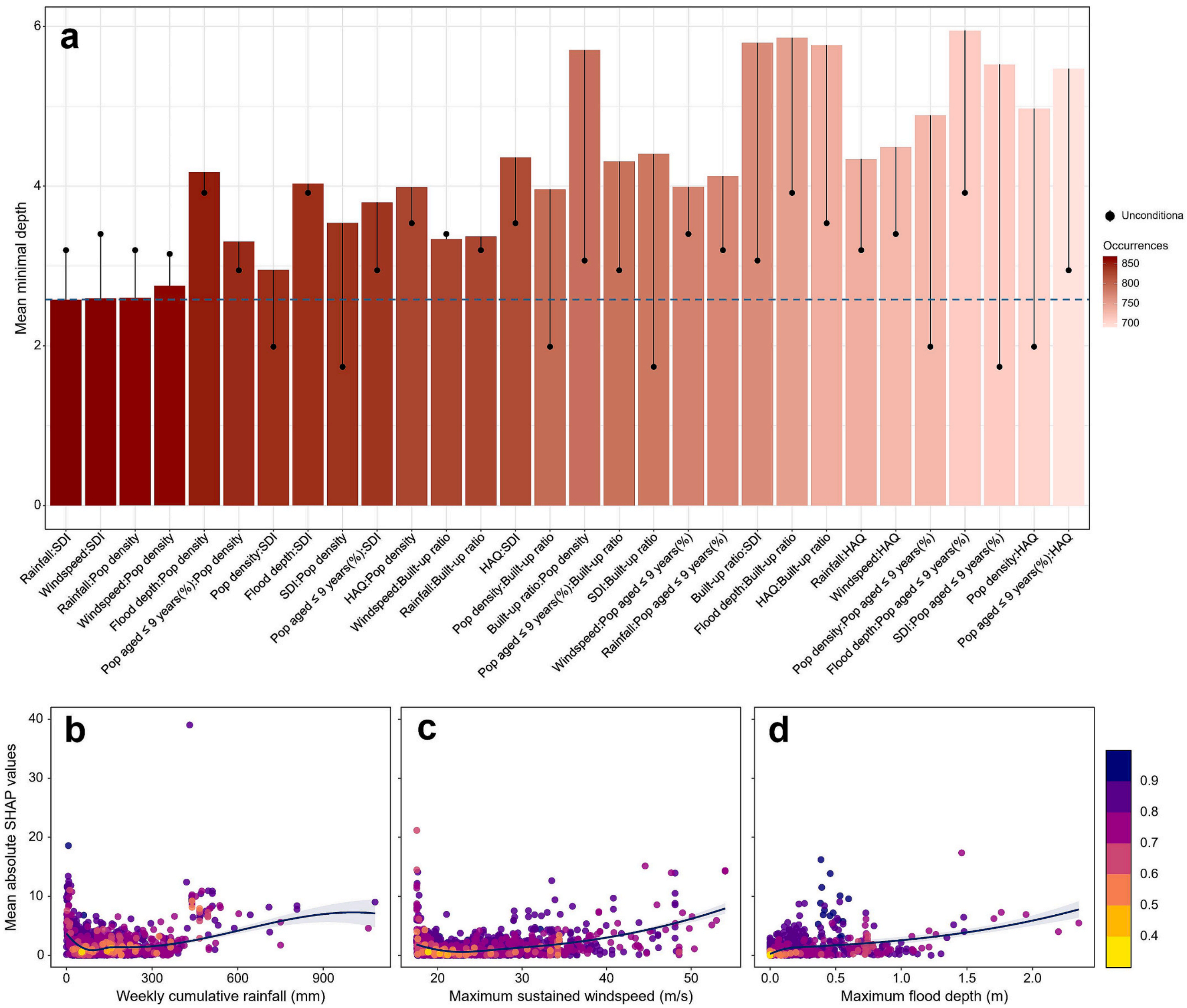

Fig. 6. Relative importance of interactions between the included potential associated factors, and the exposure-importance relationships of TC physical characteristics regarding TC-related deaths. a, pairwise interaction multiway importance among candidate factors estimated from the RFR model. Interactions are ordered by decreasing number of occurrences (indicated by depth of red). The conditional and unconditional mean minimal depth across forest trees for the 30 most frequent interactions are displayed. Unconditional minimal depth measures the average depth at which a variable is used across the forest overall. Conditional minimal depth measures the depth of a second variable strictly after the model has already split based on a first variable along the same decision path. The dashed line indicates the minimal mean conditional minimal depth. b-d, SHAP dependence plots of (b) TC-related cumulative rainfall, (c) maximum sustained windspeed, and (d) surge-driven flood depth versus their mean absolute SHAP values from the RFR model. Each point represents a single observation, colored by the SDI; the solid line shows a LOESS fit with shaded 95% CI. Abbreviations: Built-up ratio, ratio of built-up area to non-built-up area; CI, confidence interval; HAQ, healthcare access and quality index; LOESS, locally estimated scatterplot smoothing; Pop, population; rainfall, tropical cyclone-associated cumulative rainfall; RFR, random forest regression; SDI, socio-demographic index; SHAP, shapley additive explanations; TC, tropical cyclone; windspeed: tropical cyclone-associated maximum sustained windspeed.

high-resolution, real-world mortality surveillance data. By using a unified excess-mortality estimation framework, we ensure a consistent and comparable assessment of cyclone-associated mortality across countries and regions. Second, we move beyond locational or single-variable assessments by quantitatively assessing the relative importance of multiple factors simultaneously. To our knowledge, this is the first global study to systematically compare the respective explanatory contributions of TC-associated cumulative rainfall, storm surge, and maximum sustained windspeed, while controlling for economic, demographic, and locational heterogeneity. Finally, we evaluate the complex statistical interactions among physical characteristics, population traits, governance quality, healthcare accessibility, and economic development. This provides insights into how these variables jointly associate with global mortality disparities. Furthermore, the applied RFR models can account for non-linear relationships and complex interactions among variables without relying on subjectively specified non-linear parameters (e.g., degrees of freedom in spline functions) or interaction terms. (Liu et al., 2021; Ronco et al., 2023; Zhou et al., 2023) Compared to traditional meta-regression models, the RFR models can more effectively capture intricate patterns in the data and provide robust variable importance rankings of key factors associated with TC-related mortality.

Nonetheless, several limitations must be acknowledged. First, as with previous studies (Parks et al., 2022; Huang et al., 2024; Salas et al., 2024); we assessed TC exposures at the location level rather than the individual level, as obtaining individual-level data for such a large sample is impractical. The same exposures were assigned to all individuals within a location at a time, despite variations in individual TC experiences. Such nondifferential misclassification of exposures is likely to bias our estimates of TC-related mortality toward the null. (Hutcheon et al., 2010; Wei et al., 2022) In addition, studies have reported varying durations for the increased mortality following TC exposures, ranging from days (Liu et al., 2023) and weeks (Huang et al., 2025) to months (Parks et al., 2022) or even more than ten years (Young and Hsiang, 2024) following TC exposure. In this study, we limited our analysis to deaths occurring within the first two weeks after each cyclone and focused only on TC-related short-term mortality to minimise potential confounding and to avoid incorporating mortality fluctuations unlikely to be causally related to the TCs. More prolonged mortality likely arising from indirect or secondary hazards of TCs were thus not captured in this study. Identifying the short-term mortality contributors can highlight actionable targets for emergency response and preparedness, particularly in resource-limited settings where mitigation efforts are concentrated in the immediate aftermath of a TC event. Additionally, to enable global analysis, we relied on modelled TC data (windspeed, rainfall, and storm surge), which introduced inherent uncertainties and potential biases. The accuracy of the modelled exposures may vary regionally, depending on the availability of calibration data. However, our sensitivity analyses using an alternative global TC wind field dataset (ERA5-corrected wind data (Liu et al., 2025) showed that the relative importance rankings of the key variables remained robust, and that rainfall still exhibited greater relative importance than windspeed. Furthermore, it is important to note that our analysis is fundamentally exploratory and can only capture complex statistical associations rather than establish direct causal pathways. Therefore, the identified key factors should be interpreted as important factors associated with TC-related mortality rather than definitive causal mechanisms. Future work with advanced causal-inference methods to attribute long-term mortality would help to characterise the full, longer-term mortality burden and to integrate short- and long-term perspectives for policy and planning. Moreover, population displacement and dramatic shifts in environmental exposure profiles (e.g., pollutant exposure redistributions) associated with TCs could be important influential factors on the mortality. (Huang et al., 2023; Saif et al., 2024) However, to our knowledge, such data have never been systematically compiled and available on a multi-TC scale (Acosta and Irizarry, 2022), and therefore were not accounted for in the current study. To enhance our understanding of the health effects of climate and weather-related disasters, it is highly warranted to collect, compile, and incorporate richer data on these events in future studies. In addition, our RFR model achieved an out-of-bag R^2 of only 31.4% (performance on unseen data), but this is not unusually low for regression models in the context of public health research. Evidence consistently shows great variability in mortality induced by TCs, driven by numerous variables and considerable noise, which makes achieving high predictive accuracy inherently challenging. (Parks et al., 2023; Huang et al., 2024; Nethery et al., 2023) Nevertheless, this limitation may not substantially affect our findings, as the primary aim of this study was to assess the relative importance of various contextual factors rather than making predictions. (Simon et al., 2023) Furthermore, it is crucial to interpret the random forest importance metrics as indicators of relative predictive relevance within our specific set of included variables, rather than definitive measures of real-world deterministic importance. Certain specific and important factors associated with TC-related mortality such as the healthcare-seeking behaviour, effectiveness of early warning and disaster response systems, and infrastructure resilience were not incorporated in this study due to the lack of such data measured longitudinally and globally. This hinders our ability to fully disentangle the underlying mechanisms contributing to the highly variable mortality following TC events. Additionally, in our primary model, we used the point estimates of TC-related mortality from the first-stage Bayesian models as the dependent variable in the second-stage RFR model without formally propagating the estimation uncertainty. Consequently, the primary RFR model treats the estimated mortality as fixed values, which could introduce noise or lead to overconfidence in the variable importance metrics. However, our Monte Carlo sensitivity analysis demonstrated that the relative variable importance rankings remained generally stable even when this uncertainty was introduced, indicating that this unpropagated uncertainty did not substantially change our main findings. However, it should be noted that our Monte Carlo analysis assumed a normal distribution to sample the uncertainty around the first-stage mortality estimates. Given that the original Bayesian posterior distributions may exhibit asymmetry, this normal approximation might not perfectly capture the specific distributional shape of the uncertainty. Finally, despite the large sample size, the countries and territories included in this study were largely determined by data availability. We thus did not include some countries with underdeveloped data infrastructure (i.e., lacking integrated and accurate mortality data) but were potentially vulnerable to TCs (e.g., Bangladesh, Myanmar, Haiti). (Huang et al., 2023) Further work from these underrepresented regions, especially with efforts to harmonize and extend high-resolution mortality surveillance (e.g., retrospective vital-registration audits and targeted household surveys), is needed to complement the evidence provided in this study.

In summary, our analysis provided the largest to date assessment of a wide range of diverse factors associated with TC-related mortality burden, spanning TC physical characteristics, local socio-demographic conditions, governance and healthcare factors, as well as broader climatic context. The findings suggest that TC-related rainfall could be a particularly stronger global factor associated with TC-related mortality compared to TC-induced surge-driven flood depth and windspeed. Among all examined factors, socio-demographic factors were identified as the most critical factors associated with TC mortality across the globe, surpassing the relative importance of TC physical characteristics. The findings support prioritizing risk-reduction strategies that explicitly address rainfall-driven hazards, mitigate underlying socioeconomic vulnerabilities, and enhance healthcare system preparedness and resilience to effectively reduce TC-related mortality under current and future climatic scenarios.

CRediT authorship contribution statement

Wenzhong Huang: Conceptualization, Data curation, Methodology, Formal analysis, Visualization, Software, Writing – original draft. **Zhengyu Yang:** Data curation, Writing – review & editing. **Christian Otto:** Data curation, Methodology, Writing – review & editing. **Matthias Mengel:** Data curation, Methodology. **Simon Hales:** Writing – review & editing, Data curation. **Yiwen Zhang:** Writing – review & editing. **Rongbin Xu:** Writing – review & editing, Data curation. **Michelle L. Bell:** Writing – review & editing, Data curation. **Antonio Gasparrini:** Writing – review & editing, Data curation. **Haidong Kan:** Writing – review & editing, Data curation. **Francesco Sera:** Writing – review & editing, Data curation. **Joel Schwartz:** Writing – review & editing, Data curation. **Eric Lavigne:** Writing – review & editing, Data curation. **Samuel Hundessa:** Writing – review & editing. **Wenhua Yu:** Writing – review & editing, Data curation. **Paul Lester Carlos Chua:** Writing – review & editing, Data curation. **Xerxes Seposo:** Writing – review & editing, Data curation. **Patrick Goodman:** Writing – review & editing, Data curation. **Ariana Zeka:** Writing – review & editing, Data curation. **Masahiro Hashizume:** Writing – review & editing, Data curation. **Micheline S. Z. S. Coelho:** Writing – review & editing, Data curation. **Zhihu Xu:** Writing – review & editing, Data curation. **Tingting Ye:** Writing – review & editing, Data curation. **Pei Yu:** Data curation. **Yao Wu:** Data curation. **Bo Wen:** Data curation. **Yanming Liu:** Writing – review & editing, Data curation. **Shanshan Li:** Conceptualization, Writing – review & editing, Data curation. **Yuming Guo:** Conceptualization, Supervision, Project administration, Funding acquisition, Writing – review & editing, Data curation.

Declaration of competing interest

The authors declare the following financial interests/personal relationships which may be considered as potential competing interests: Given his role as Editor, Yuming had no involvement in the peer review of this article and had no access to information regarding its peer review. Full responsibility for the editorial process for this article was delegated to another journal editor. If there are other authors, they declare that they have no known competing financial interests or personal relationships that could have appeared to influence the work reported in this paper.

Acknowledgements

This work was supported by the Australian Research Council (DP210102076) and the Australian National Health & Medical Research Council (APP2000581). W.H., T.Y., Y.W., B.W., and K.J. were supported by China Scholarship Council funds (numbers 202006380055, 201906320051, 202006010044, 202006010043 and 202006240087). Z.Y. and W.Y. were supported by a Monash Graduate Scholarship and a Monash International Tuition Scholarship. Y.Z. was supported by the NHMRC e-Asia Joint Research Program Grant (GNT2000581). R.X. was supported by the VicHealth Postdoctoral Research Fellowships 2022. K. T. was supported by the National Research Council of Thailand (NRCT): E-Asia Joint Research Program: Climate change impact on natural and human systems (N33A650979). P.Y. was supported by Monash Faculty of Medicine Nursing and Health Science (FMNHS) Early Career Postdoctoral Fellowships 2023. S.L. by an Emerging Leader Fellowship (GNT2009866) of the Australian National Health and Medical Research Council; Y.G. by Leader Fellowship (GNT2008813) of the Australian National Health and Medical Research Council.

Appendix A. Supplementary data

Supplementary data to this article can be found online at https://doi.org/10.1016/j.envint.2026.110409.

Data availability

The authors do not have permission to share data.

References

CRED. EM-DAT The International Disaster Database.
Knutson, T., Camargo, S.J., Chan, J.C.L., Emanuel, K., Ho, C.-H., Kossin, J., et al., 2020. Tropical cyclones and climate change assessment: part II: projected response to anthropogenic warming. Bull. Am. Meteorol. Soc. 101 (3), E303–E322.
Wang, G., Wu, L., Mei, W., Xie, S.P., 2022. Ocean currents show global intensification of weak tropical cyclones. Nature 611 (7936), 496–500.
Reimann, L., Vafeidis, A.T., Honsel, L.E., 2023. Population development as a driver of coastal risk: current trends and future pathways. Cambridge Prisms: Coastal Futures 1, e14.
Parks, R.M., Kontis, V., Anderson, G.B., Baldwin, J.W., Danaei, G., Toumi, R., et al., 2023. Short-term excess mortality following tropical cyclones in the United States. Sci. Adv. 9 (33), eadg6633.
Young, R., Hsiang, S., 2024. Mortality caused by tropical cyclones in the United States. Nature 635 (8037), 121–128.
Huang, W., Li, S., Vogt;, T., Xu, R., Tong, S., Molina, T., et al., 2023. Global short-term mortality risk and burden associated with tropical cyclones from 1980 to 2019: a multi-country time-series study. Lancet Planet Health. 7 (8), e694–e705.
Huang, W., Yang, Z., Zhang, Y., Vogt;, T., Armstrong, B., Yu, W., et al., 2024. Tropical cyclone-specific mortality risks and the periods of concern: a multicountry time-series study. PLoS Med. 21 (1), e1004341.
Parks, R.M., Benavides, J., Anderson, G.B., Nethery, R.C., Navas-Acien, A., Dominici, F., et al., 2022. Association of tropical cyclones with county-level mortality in the US. J. Am. Med. Assoc. 327 (10), 946–955.
Parks, R.M., Anderson, G.B., Nethery, R.C., Navas-Acien, A., Dominici, F., Kioumourtzoglou, M.A., 2021. Tropical cyclone exposure is associated with increased hospitalization rates in older adults. Nat. Commun. 12 (1), 1545.
Huang, W., Vogt;, T., Park, J., Yang, Z., Ritchie, E.A., Xu, R., et al., 2024. Risks of infectious disease hospitalisations in the aftermath of tropical cyclones: a multi-country time-series study. Lancet Planet Health. 8 (9), e629–e639.
Salas, R.N., Burke, L.G., Phelan, J., Wellenius, G.A., Orav, E.J., Jha, A.K., 2024. Impact of extreme weather events on healthcare utilization and mortality in the United States. Nat. Med. 30 (4), 1118–1126.
Prada, D., Baccarelli, A.A., Kupsco, A., Parks, R.M., 2024. Climate change and health: understanding mechanisms will inform mitigation and prevention strategies. Nat. Med. 30 (6), 1522–1524.
Jing, R., Heft-Neal, S., Chavas, D.R., Griswold, M., Wang, Z., Clark-Ginsberg, A., et al., 2024. Global population profile of tropical cyclone exposure from 2002 to 2019. Nature 626 (7999), 549–554.
Geiger, T., Gütschow, J., Bresch, D.N., Emanuel, K., Frieler, K., 2021. Double benefit of limiting global warming for tropical cyclone exposure. Nat. Clim. Chang. 11 (10), 861–866.
Ye, M., Wu, J., Liu, W., He, X., Wang, C., 2020. Dependence of tropical cyclone damage on maximum wind speed and socioeconomic factors. Environ. Res. Lett. 15 (9), 094061.
Geiger, T., Frieler, K., Bresch, D., 2018. A global historical data set of tropical cyclone exposure (TCE-DAT). Earth Syst. Sci. Data 10, 185–194.
Huang, W., Xu, R., Yang, Z., Otto, C., Hales, S., Hundessa, S., et al., 2025. Cause specific mortality risks associated with tropical cyclones in multiple countries and territories: two stage, time series study. BMJ 391, e084906.
Tennant, E., Gilmore, E.A., 2020. Government effectiveness and institutions as determinants of tropical cyclone mortality. PNAS 117 (46), 28692–28699.
Huang, W., Gao, Y., Xu, R., Yang, Z., Yu, P., Ye, T., et al., 2023. Health effects of cyclones: a systematic review and meta-analysis of epidemiological studies. Environ. Health Perspect. 131 (8), 86001.
Gasparrini, A., Vicedo-Cabrera, A.M., Tobias, A., 2024. The multi-country multi-city collaborative research network: an international research consortium investigating environment, climate, and health. Environ. Epidemiol. 8 (5), e339.
Doocy, S., Dick, A., Daniels, A., Kirsch, T.D., 2013. The human impact of tropical cyclones: a historical review of events 1980-2009 and systematic literature review. PLoS Curr. 5.
Dobson, J.E., Bright, E.A., Coleman, P.R., Durfee, R.C., Worley, B.A., 2000. LandScan: a global population database for estimating populations at risk. Photogramm. Eng. Remote Sens. 66 (7), 849–857.
Xu, R., Ye, T., Yue, X., Yang, Z., Yu, W., Zhang, Y., et al., 2023. Global population exposure to landscape fire air pollution from 2000 to 2019. Nature 621 (7979), 521–529.
Holland, G.J., Belanger, J.I., Fritz, A., 2010. A revised model for radial profiles of hurricane winds. Mon. Weather Rev. 138 (12), 4393–4401.
Peduzzi, P., Chatenoux, B., Dao, H., De Bono, A., Herold, C., Kossin, J., et al., 2012. Global trends in tropical cyclone risk. Nat. Clim. Chang. 2 (4), 289–294.
Lange, S., Volkholz, J., Geiger, T., Zhao, F., Vega, I., Veldkamp, T., et al., 2020. Projecting exposure to extreme climate impact events across six event categories and three spatial scales. Earth's Future 8 (12), e2020EF001616.
Knapp, K.R., Kruk, M.C., Levinson, D.H., Diamond, H.J., Neumann, C.J., 2010. The international best track archive for climate stewardship (IBTrACS) unifying tropical cyclone data. Bull. Am. Meteorol. Soc. 91 (3), 363–376.
Zhu, L., Quiring, S.M., Emanuel, K.A., 2013. Estimating tropical cyclone precipitation risk in Texas. Geophys. Res. Lett. 40 (23), 6225–6230.
Frieler, K., Volkholz, J., Lange, S., Schewe, J., Mengel, M., del Rocío Rivas López, M., et al., 2024. Scenario setup and forcing data for impact model evaluation and impact attribution within the third round of the Inter-Sectoral Impact Model Intercomparison Project (ISIMIP3a). Geosci. Model Dev. 17 (1), 1–51.
Vogt;, T., Treu, S., Mengel, M., Frieler, K., Otto, C., 2024. Modeling surge dynamics improves coastal flood estimates in a global set of tropical cyclones. Commun. Earth Environ. 5 (1), 529.
Massarra, C.C., Friedland, C.J., Marx, B.D., Dietrich, J.C., 2019. Predictive multi-hazard hurricane data-based fragility model for residential homes. Coast. Eng. 151, 10–21.
Hermans, T.H.J., Busecke, J.J.M., Wahl, T., Malagón-Santos, V., Tadesse, M.G., Jane, R. A., et al., 2024. Projecting changes in the drivers of compound flooding in Europe using CMIP6 models. Earth's Future 12 (5), e2023EF004188.
Kontis, V., Bennett, J.E., Rashid, T., Parks, R.M., Pearson-Stuttard, J., Guillot, M., et al., 2020. Magnitude, demographics and dynamics of the effect of the first wave of the COVID-19 pandemic on all-cause mortality in 21 industrialized countries. Nat. Med. 26 (12), 1919–1928.
Ebi, K.L., 2024. Weekly temperature data are sufficient to estimate exposure-response relationships: a boon for health adaptation in low-resource settings. Lancet Reg Health Eur. 36, 100811.
Nethery, R.C., Katz-Christy, N., Kioumourtzoglou, M.A., Parks, R.M., Schumacher, A., Anderson, G.B., 2023. Integrated causal-predictive machine learning models for tropical cyclone epidemiology. Biostatistics 24 (2), 449–464.
Graefe, A., Küchenhoff, H., Stierle, V., Riedl, B., 2015. Limitations of ensemble bayesian model averaging for forecasting social science problems. Int. J. Forecast. 31 (3), 943–951.
Liu, M., Hu, S., Ge, Y., Heuvelink, G.B.M., Ren, Z., Huang, X., 2021. Using multiple linear regression and random forests to identify spatial poverty determinants in rural China. Spatial Stat. 42, 100461.
Ronco, M., Tárraga, J.M., Muñoz, J., Piles, M., Marco, E.S., Wang, Q., et al., 2023. Exploring interactions between socioeconomic context and natural hazards on human population displacement. Nat. Commun. 14 (1), 8004.
Zhou, Z., Qiu, C., Zhang, Y., 2023. A comparative analysis of linear regression, neural networks and random forest regression for predicting air ozone employing soft sensor models. Sci. Rep. 13 (1), 22420.
Tibshirani J, Athey S, Friedberg R, Hadad V, Hirshberg D, Miner L, et al. grf: Generalized random forests. 2025.

Paluszynska A, Biecek P, Jiang Y. randomForestExplainer: Explaining and visualizing random forests in terms of variable importance. R package version 09. 2017.
König G, Molnar C, Bischl B, Grosse-Wentrup M, editors. Relative Feature Importance. 2020 25th International Conference on Pattern Recognition (ICPR); 2021 10-15 Jan. 2021.
Lundberg, S.M., Erion, G., Chen, H., DeGrave, A., Prutkin, J.M., Nair, B., et al., 2020. From local explanations to global understanding with explainable AI for trees. Nat. Mach. Intell. 2 (1), 56–67.
Deng, Y., Jiang, W., Ling, Z., Liu, L., Sun, S., 2025. Revealing the driving factors of urban wetland park cooling effects using Random Forest regression and SHAP algorithm. Sustain. Cities Soc. 120, 106151.
Lundberg SM, Lee S-I. A unified approach to interpreting model predictions. Proceedings of the 31st International Conference on Neural Information Processing Systems; Long Beach, California, USA: Curran Associates Inc.; 2017. p. 4768–77.
Voges, L.F., Jarren, L.C., Seifert, S., 2023. Exploitation of surrogate variables in random forests for unbiased analysis of mutual impact and importance of features. Bioinformatics 39 (8).
Liu, G., Jiang, S., Zheng, M., Lin, S., Kong, Y., Zhan, P., 2025. A global ERA5-based tropical cyclone wind field dataset enhanced by integrated parametric correction methods. Sci. Data 12 (1), 1429.
Lindgren, F., Rue, H., 2015. Bayesian spatial modelling with R-INLA. J. Stat. Softw. 63 (19), 1–25.
Breiman, L., Cutler, A., Liaw, A., Wiener, M., 2018. Package 'Randomforest'. University of California, Berkeley, Berkeley, CA, USA.
Liu, Y., Yan, M., Du, H., Sun, Q., Anderson, G.B., Li, T., 2023. Increased mortality risks from a spectrum of causes of tropical cyclone exposure - China, 2013-2018. China CDC Wkly. 5 (6), 119–124.
Dresser, C., Allison, J., Broach, J., Smith, M.E., Milsten, A., 2016. High-amplitude atlantic hurricanes produce disparate mortality in small, low-income countries. Disaster Med. Public Health Prep. 10 (6), 832–837.
Rappaport, E.N., 2014. Fatalities in the United States from atlantic tropical cyclones: new data and interpretation. Bull. Am. Meteorol. Soc. 95 (3), 341–346.
Bosma, C.D., Wright, D.B., Nguyen, P., Kossin, J.P., Herndon, D.C., Shepherd, J.M., 2020. An intuitive metric to quantify and communicate tropical cyclone rainfall hazard. Bull. Am. Meteorol. Soc. 101 (2), E206–E220.
Bosma, C.D., Wright, D.B., Nguyen, P., Kossin, J.P., Herndon, D.C., Shepherd, J.M., 2020. Extreme rainfall multiplier: an intuitive metric for tropical cyclone hazards. Bull. Am. Meteorol. Soc. 101 (3), 215–220.
He, C., Breitner-Busch, S., Huber, V., Chen, K., Zhang, S., Gasparrini, A., et al., 2024. Rainfall events and daily mortality across 645 global locations: two stage time series analysis. BMJ 387, e080944.
Yang, Z., Huang, W., McKenzie, J.E., Xu, R., Yu, P., Ye, T., et al., 2023. Mortality risks associated with floods in 761 communities worldwide: time series study. BMJ 383, e075081.
Vosper, E., Watson, P., Harris, L., McRae, A., Santos-Rodriguez, R., Aitchison, L., et al., 2023. Deep learning for downscaling tropical cyclone rainfall to hazard-relevant spatial scales. J. Geophys. Res. Atmos. 128 (10), e2022JD038163.
Wolkin, A., Patterson, J.R., Harris, S., Soler, E., Burrer, S., McGeehin, M., et al., 2015. Reducing public health risk during disasters: identifying social vulnerabilities. J Homel Secur Emerg Manag. 12 (4), 809–822.
Pratiti, R., 2023. An ecological approach to disaster mitigation: a literature review. Cureus 15 (9), e45500.
Hutcheon, J.A., Chiolero, A., Hanley, J.A., 2010. Random measurement error and regression dilution bias. BMJ 340, c2289.
Wei, Y., Qiu, X., Yazdi, M.D., Shtein, A., Shi, L., Yang, J., et al., 2022. The impact of exposure measurement error on the estimated concentration-response relationship between long-term exposure to PM2.5 and mortality. Environ. Health Perspect. 130 (7), 77006.
Saif, U., Aysun, U.G., Scott, W.F., Montaha, B., Nazima, H., Isik, F., et al., 2024. Climate change - mediated atmospheric 210Po and 210Pb distribution: how significant can it be for the inhalation dose to humans? J. Environ. Exposure Asses. 3 (1), 3.
Acosta, R.J., Irizarry, R.A., 2022. A flexible statistical framework for estimating excess mortality. Epidemiology 33 (3), 346–353.
Simon, S.M., Glaum, P., Valdovinos, F.S., 2023. Interpreting random forest analysis of ecological models to move from prediction to explanation. Sci. Rep. 13 (1), 3881.